Schweizerischer Erdbebendienst
Service Sismologique Suisse
Servizio Sismico Svizzero
Servizi da Terratrembels Svizzer

ETH
Eidgenössische Technische Hochschule Zürich
Swiss Federal Institute of Technology Zurich

EPFL (SEPFL)

SITE CHARACTERIZATION REPORT

Clotaire MICHEL, Valerio POGGI, Daniel ROTEN,

Jan BURJANEK, Carlo CAUZZI, Donat FÄH

Sonneggstrasse 5 CH-8092 Zürich Switzerland; E-mail: clotaire.michel@sed.ethz.ch

Last modified : October 15, 2013

Abstract

Site characterization using active seismics and ambient vibration measurements were performed on the EPFL campus in Lausanne. The station SEPFL of the Swiss Strong Motion Network was installed in 2011. In order to characterize the velocity profile under the station, existing geotechnical and geophysical data collected for a microzonation study as well as new geophysical data were used. Particularly, a $46\,\mathrm{m}$ long seismic line was performed. These investigations showed that the velocity profiles have 5 first meters with low velocity, around $130 - 140\,\mathrm{m/s}$. A second layer from 5 to $10\,\mathrm{m}$ has slightly higher velocities around $200\,\mathrm{m/s}$. Finally, the layer down to $25\,\mathrm{m}$ shows relatively homogeneous velocities around $275\,\mathrm{m/s}$. Below $25\,\mathrm{m}$, this velocity may increase gradually down to the bedrock, located at $37\,\mathrm{m}$. $V_{s,30}$ is found to be $224\,\mathrm{m/s}$. These profiles are close to the models used for microzonation of the EPFL site. The theoretical SH transfer function and impedance contrast of the quarter-wavelength velocity computed from the inverted profiles support a large amplification up to a factor of 10 at the resonance frequencies, especially the fundamental frequency at $1.9\,\mathrm{Hz}$. Recordings on the new station will allow to validate these simple models.

Contents

1 Introduction

The station SEPFL (Lausanne EPFL) is part of the Swiss Strong Motion Network (SSMNet) in the Canton Vaud. SEPFL has been installed in the framework of the SSMNet Renewal project in 2011. This project includes also the site characterization. Active seismics has been selected for this task at this site. Detailed geological, geotechnical and geophysical data were already available at this site where a microzonation study was performed [Résonance, 2006]. In addition, active seismics and single station measurements were performed at the station site. This station is located on loose lacustrine sediments on top of moraine. This report presents the measurement setups, the H/V results and of the seismic processing of the surface waves (dispersion curves). Then, an inversion of these results for a velocity profile is performed. Standard parameters are derived to evaluate the amplification at this site.

Canton	City	Location	Station code	Site type	Slope
Vaud	Lausanne	EPFL	SEPFL	Lacustrine sediments	Flat

Table 1: Main characteristics of the study-site.

Figure 1: Picture of the site.

2 Geology and geotechnics

For the spectral microzonation of EPFL [Résonance, 2006], the De Cerenville company made a detailed geological and geotechnical study of the EPFL site, including borehole investigations that are summarized in the following.

Silty glaciolacustrine deposits (named A) can be found at the surface with increasing thickness to the North. According to the map of this layer, at the station site, it is $17\,\mathrm{m}$ thick, $18\,\mathrm{m}$ thick at the active seismic experiment site. Below this layer, a non-consolidated moraine with silt, sand and some gravels (named B) can be found, irregularly in space. Its thickness is $8\,\mathrm{m}$ and $7\,\mathrm{m}$ for the station and the active seismic experiment sites, respectively. A compacted moraine (named C) is present below with a thickness of $12\,\mathrm{m}$ and $13\,\mathrm{m}$ for the station and the active seismic experiment sites, respectively. Finally, the bedrock (named D) is made of a molasse from the Chattian Age with marls and sandstones, consequently at 37 and $38\,\mathrm{m}$ depth, respectively.

The ground water table was at $3\,\mathrm{m}$ below the surface at the station site in 1971.

Layer	**Depth m**	**Density kg/m^3**	**Frict. angle** $\phi\,^\circ$	**Coh. c' kN/m^2**	**Undrained Coh.** c_u **kN/m^2**	**Elasticity mod. E MPa**	N_{SPT} **/30cm**
A	0	2000	27	4	20	4-8	4-7
B	17	2000	27	6	22	6-8	6-10
C	25	2200	33	30	150	40-120	50-70
D	37	2500	-	-	-	1500-5000	-

Table 2: Geotechnical characteristics of the soil column under station SEPFL (De Cerenville, 2006).

Using these parameters and the theoretical formula for the shear wave velocity : $V_s(E) = \sqrt{\frac{G}{\rho}} = \sqrt{\frac{E}{2(1+\nu)\rho}}$, we can deduce the corresponding $V_s(E)$ in each layer (Tab. 3). The results are not relevant since much higher velocities are awaited.

Moreover, using Ohta and Goto [1978] empirical formula $V_s(N) = 68.79 \times N^{0.171} \times H^{0.199} \times E \times F$, with H the depth, N the SPT number for 30 cm penetration, E being 1 for Holocene soils, 1.303 for Pleistocene deposits and F from 1 to 1.15 depending on the soil type (excepted gravels, that is not present in this profile), one can extract velocity values that are closer to the expectations (Tab. 3).

Layer	$V_s(E)$ **m/s**	$V_s(N)$ **m/s**
A	25-40	100-185
B	30-40	230-290
C	80-160	330-440
D	520-1020	-

Table 3: Shear wave velocity in each layer deduced from the geotechnical measurements based on 2 different parameters (E the Young's modulus and N the SPT count)

3 Experiment description

3.1 Sources

The ground surface is permanently subjected to ambient vibrations due to:

- natural sources (ocean and large-scale atmospheric phenomena) below $1\,\mathrm{Hz}$,
- local meteorological conditions (wind and rain) at frequencies around $1\,\mathrm{Hz}$,
- human activities (industrial machines, traffic...) at frequencies above $1\,\mathrm{Hz}$ [Bonnefoy-Claudet et al., 2006].

The objective of so called H/V measurements is to record these ambient vibrations and to use the polarization of the recorded waves (H/V ratio) to derive the resonance frequencies of the soil column.

Moreover, active seismic experiments were performed. Two types of artificial sources have been employed, with the aim of assessing their possibilities and limitations; as first it was used a weight drop system with a mass of $120\,\mathrm{kg}$, dropping from an height up to $2\,\mathrm{m}$ ($1.13\,\mathrm{m}$ used in this experiment) (Fig. 2). Subsequently, a sledge hammer was tested. In addition, data from Geo2X company using 200 g explosives [Résonance, 2006] were re-processed. The objective of the measurements is to record the produced vibrations and to use their propagation properties to infer the underground structure. The phase delays at many different stations are used to derive the velocity of surface waves at different frequencies (dispersion). The dispersion curves are then used to derive the properties of the soil column using an inversion process.

Figure 2: The 120kg dropping mass device which has been used as artificial source to stimulate the generation of Rayleigh waves.

3.2 Equipment

For H/V measurements, a Quanterra Q330 datalogger with Lennartz 3C 5 s seismometer were used (see Tab. 4). The time stamps was not synchronized on GPS and may suffer from a shift of several seconds (or more). The sensor is placed directly on the ground (generally road) and leveled using the screws.

For the active seismic measurements, 24 three-component geophones (4.5Hz corner frequency) were used (see Tab. 4) and 3 Geode dataloggers connected together for time synchronization. Channels 1/2/3 correspond respectively to Transverse/Longitudinal/Vertical directions.

Digitizer	Model	Number	Resolution
	Quanterra Q330	1	24 bits
	Geode	3	24 bits
Sensor type	**Model**	**Number**	**Cut-off frequency**
Seismometer	Lennartz 3C 5s	1	0.2 Hz
Geophone	?	24	4.5 Hz

Table 4: Equipment used.

3.3 Geometry of the experiment

H/V measurements were performed by Resonance on the whole EPFL campus (Fig. 7). In addition, test measurements to find a new location for the strong motion station SEPFL were performed in two locations and a single station measurement at the final location of the station was performed.

Active seismic lines were also performed by the Geo2X company for Resonance at 2 locations on the campus (Fig. 7). Profile 1 is representative of the glaciolacustrine deposits with similar characteristics compared to the SEPFL station location. The seismic lines includes 48 geophones with $4\,\mathrm{m}$ inter-distance. We performed an additional line at the SEPFL station location. The performed seismic line includes 24 geophones with $2\,\mathrm{m}$ inter-distance (total of $46\,\mathrm{m}$) (Fig. 3). The final usable datasets are detailed in appendix.

3.4 Positioning of the stations

For these measurements, the positioning of the stations was done by picking points on Google Earth. It allows a positioning with an accuracy of about $2\,\mathrm{m}$.

4 Data quality

For the single station data, only the recordings in the 3 points performed by SED were available for processing. For the active seismic data, both lines performed by the Geo2X company and SED are available for (re-)processing.

Figure 3: Location of the seismic line (in red) and of the two source locations A and B (red stars).

4.1 Geo2X dataset

Geo2X performed 2 shots of explosives at 2 locations: Profile 1 is representative for glaciolacustrine deposits, similar to the SEPFL station location and reprocessed in the following; Profile 2 is representative for moraine and not included here. It seems that a filter at 25 Hz was used for profile 1, which makes impossible the processing above this value.

4.2 SED dataset

Four groups of wave-field excitations of 7 to 12 shots each were performed on the two ends of the line (A and B in Fig. 3). Unfortunately, source location A didn't provide any reliable result, probably because of the heterogeneity of the sub-soil structure and the presence of the nearby building, which prevented from the generation of a coherent surface wave-field. This also invalidated the comparison between the two source types, which was performed in location A. In the following, therefore, only the results from source location B will be considered as reliable.

For each wave-field excitation a recording of about 2 seconds was performed. For the processing, then, the consecutive recordings have been merged in a unique continuous stream of data (e.g. Fig. 4). However, not all the shots were identically successful during the experiment. Therefore, a further selection on the quality of the performed wave-field excitation has been performed. As such, only the best shots were selected and gathered into a continuous stream.

Several problems were experienced with automatic triggering. For unknown reason, it was not possible to correctly synchronize the shot time with measurements. Therefore, some recordings were performed by manually triggering the start time. This is generally not a problem for surface wave analysis, since only relative time-differences between couple of receivers are used, but it prevents from using any other type of technique based on the analysis of the absolute travel-time (reflection or refraction seismics). Finally, some channels of the three components

sensors didn't work properly during acquisition (see next paragraph), and they were consequently not considered in the elaboration.

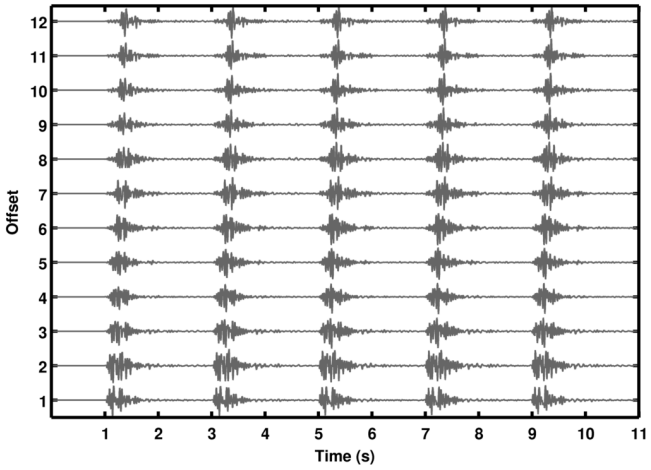

Figure 4: Example of continuous stream of shots obtained by using the 120kg mass source (here source location A, channel 2, shots 41-46).

Detailed information about these active recordings can be found in the appendix.

5 H/V processing

5.1 Processing methods

Recordings were processed using the classical H/V method. In this method, the ratios of the smoothed Fourier Transform of selected time windows are averaged. Tukey windows (cosine taper of 5% width) of 50 s long overlapping by 50% were selected. Konno and Ohmachi [1998] smoothing procedure with b=60 was used.

5.2 Results in EPFL

The H/V spectral ratios computed at the test station XLAU1 and at the final SEPFL station site are very similar (Fig. 5), with a peak at 2.15 and 1.93 Hz, respectively (Fig. 6). Fig. 7 provides the resonance frequencies mapped by Résonance [2006], with values between 1.5 and 3.5 Hz on the EPFL campus, 2 Hz close to the station site, in agreement with SED measurements. No correlation can be shown with the bedrock depth, but a correlation with the interface between glaciolacustrine sediments and moraine is highlighted in Résonance [2006] (Fig. 7).

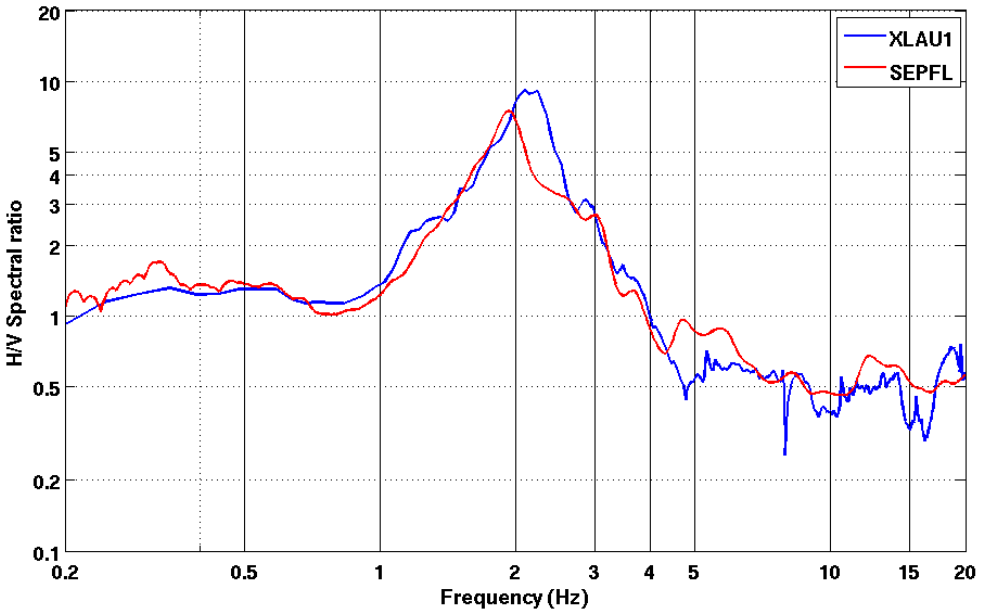

Figure 5: H/V spectral ratios at test station XLAU1 and at final site for station SEPFL.

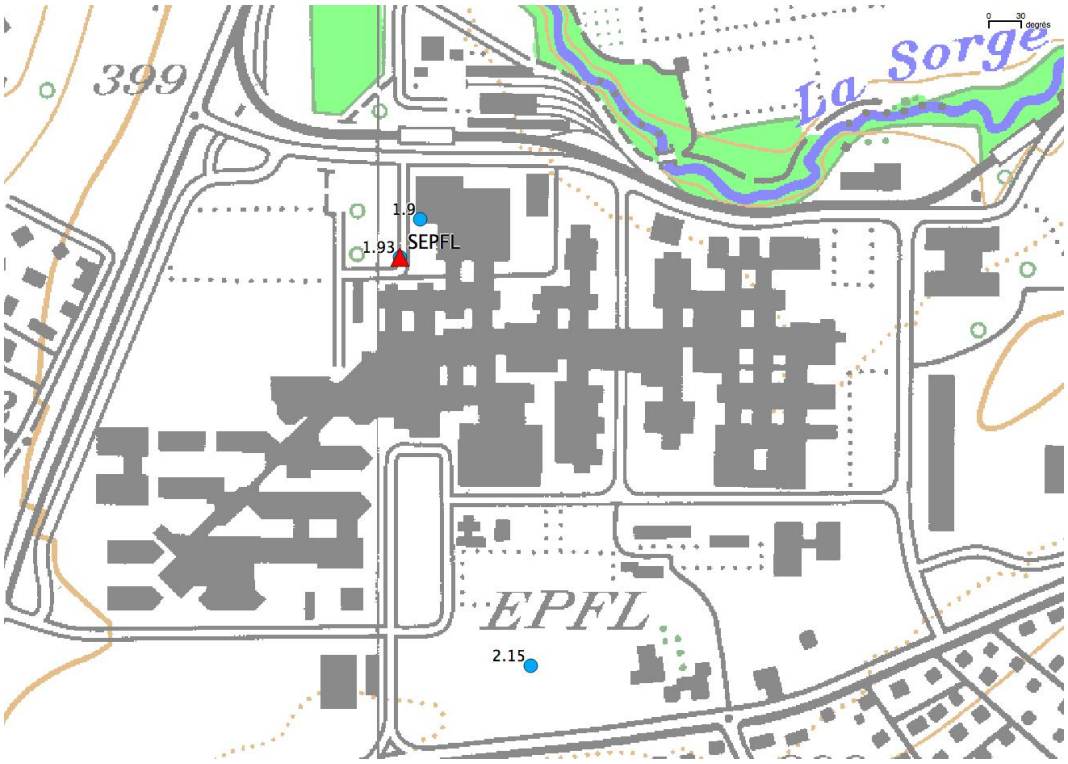

Figure 6: Single station measurements performed by SED (blue points) with resonance frequency.

Figure 7: H/V points performed by Resonance (red crosses), SEPFL seismic station and active seismic lines (blue).

6 Seismic processing

6.1 Processing methods and parameters

For the Geo2X data, the vertical component was processed using the classical f-k approach and the t-f-k analysis [Poggi et al., 2012].

For the SED data, the vertical (channel 3) and the radial (channel 2) directions of recording have been processed using the classical f-k approach and the t-f-k analysis [Poggi et al., 2012]. The transverse direction was processed, but the results have not been included in this report, since the employed sources do not give the possibility to directly generate anti-plane motion, and it is consequently not possible to rely on those results. Therefore, the following considerations are representative of Rayleigh-wave dispersion only.

6.2 Obtained dispersion curves

For the Geo2X data, results are presented in Fig. 8. The results using the two approaches are comparable.

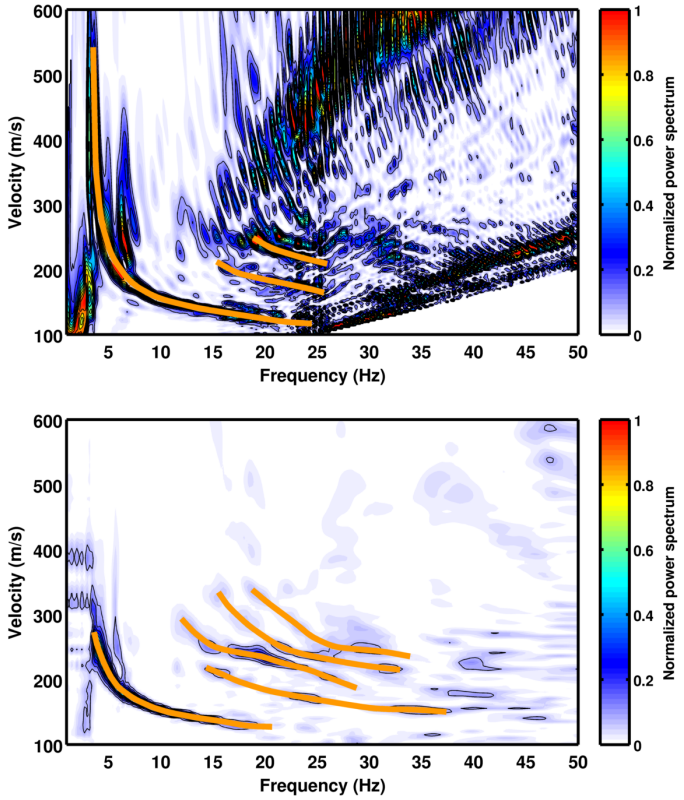

Figure 8: Results from the acquisition survey performed by Geo2X (profile 1 - glaciolacustrine). In A using Classic F-K processing, in B using the wavelet T-F-K method. The fundamental mode is clearly visible and can be tracked from a frequency of 4Hz up to 20Hz. Unfortunately, recordings were strongly filtered above 25Hz, which make difficult the elaboration at high frequencies.

For the SED data, several surface wave modes are clearly identifiable in the velocity-frequency plane (e.g. Fig. 9 and Fig. 10). A maximum in the spectrum can also be identified in the range 10 to 15Hz and rather low velocities. This might correspond to the fundamental mode of Rayleigh waves, which is not sufficiently excited by using the available source to be visible along the whole frequency range of elaboration. This creates some ambiguity in addressing the mode number of the higher modes. However, the presence of this mode is confirmed by the results of the Geo2X in the site "glaciolacustrine" (Fig. 8).

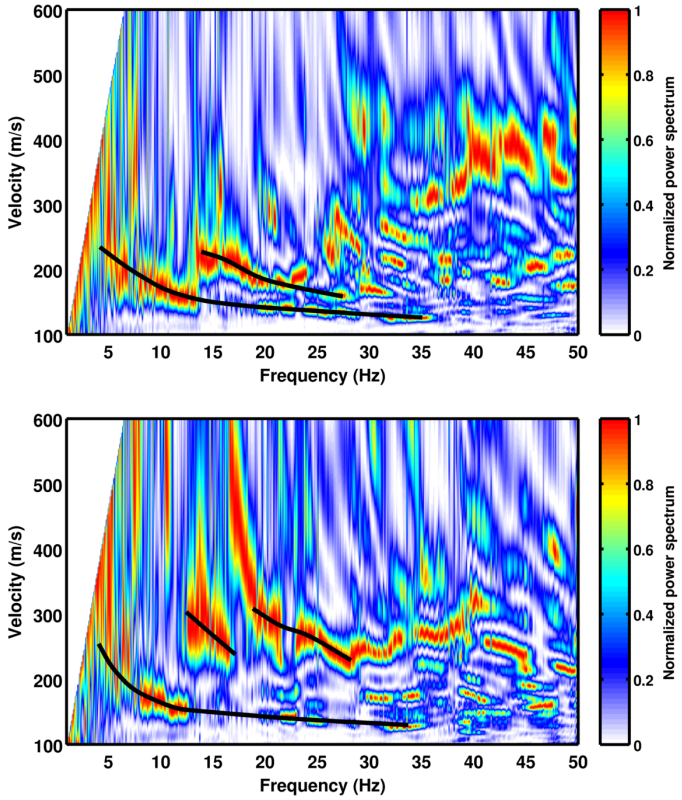

Figure 9: Result for the shot location A using classic F-K processing on the vertical (top) and horizontal-radial (bottom) direction. Few parts the dispersion curves can be identify and reliably addressed to a give mode.

6.3 Interpretation

The definition of the final dispersion model required some manual interpretation. This was done by cross-comparing the results from different elaborations and datasets (e.g. Fig. 11). To avoid bias in the definition of the final velocity model, the modal interpretation was then performed in a rather conservative way. Only those modes which appeared to be well defined and could be tracked between different elaborations were considered and included in the interpretation. The result is a three modes model, which spans a velocity range between about 120m/s and 300m/s (Fig. 12).

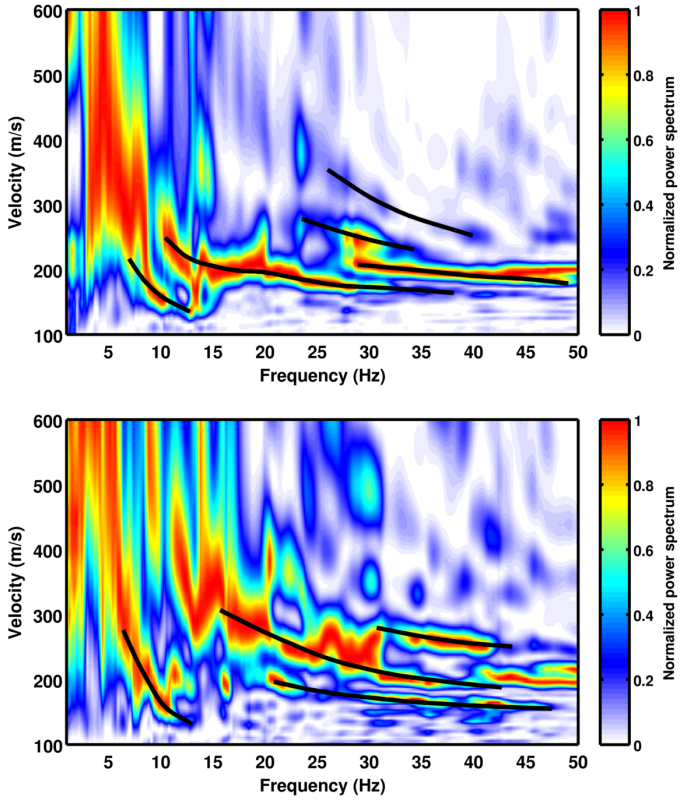

Figure 10: Result for the shot location B using wavelet T-F-K processing on vertical (top) the horizontal-radial (bottom) direction. Few modes can be identify, even if it is impossible to track the fundamental mode at high frequencies.

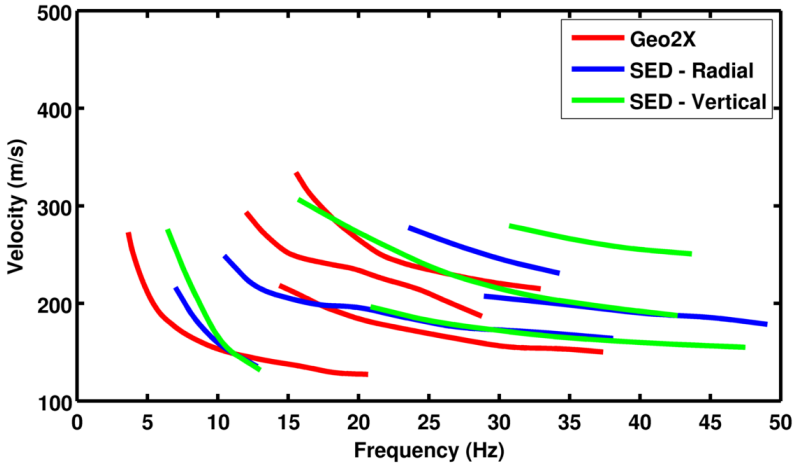

Figure 11: Example comparison between the picked modes from the different datasets. Note that the results from Geo2X profile 1 are not fully comparable to our results, since the two measurements locations differ in few hundreds of meters.

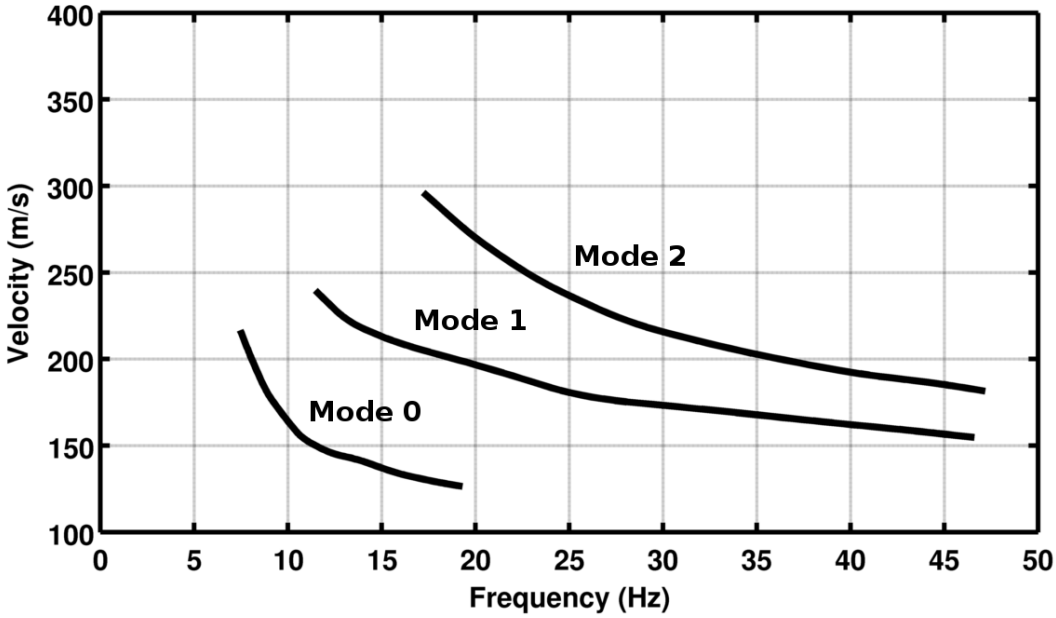

Figure 12: The final modal interpretation which will be used for the inversion.

7 Inversion and interpretation

7.1 Inversion

For the inversion, the 3 Rayleigh modes dispersion curves were used as simultaneous targets without standard deviation to avoid different weighting as well as the right flank of the H/V curve with weight 0.3 and the resonance frequency at the SEPFL station site $1.9\,\mathrm{Hz}$ with weight 0.1. All curves were resampled using 50 points between 1.8 and $50\,\mathrm{Hz}$ in log scale.

The inversion was performed using the Improved Neighborhood Algorithm (NA) [Wathelet, 2008] implemented in the Dinver software. In this algorithm, the tuning parameters are the following: Ns_0 is the number of starting models, randomly distributed in the parameter space, Nr is the the number of best cells considered around these Ns_0 models, Ns is the number of new cells generated in the neighborhood of the Nr cells (Ns/Nr per cell) and It_{max} is the number of iteration of this process. The process ends with $Ns_0 + Nr * \frac{Ns}{Nr} * It_{max}$ models. The used parameters are detailed in Tab. 5.

It_{max}	Ns_0	Ns	Nr
500	10000	100	100

Table 5: Tuning parameters of Neighborhood Algorithm.

During the inversion process, low velocity zones were not allowed. The Poisson ratio was inverted in each layer in the range 0.2-0.4 and the density was fixed according to the geotechnical study between 2000 and $2500\,\mathrm{kg/m^3}$. Inversions with free layer depths as well as fixed layer depths were performed. For the fixed layer depth, the layering proposed by the geotechnics was followed and the bedrock depth and velocity were fixed at $37\,\mathrm{m}$ and $1500\,\mathrm{m/s}$. Trials without fixing these values were also performed but the geophysical data do not constrain the bedrock depth and velocity. The smooth ellipticity curve leads to a smooth gradient in the bedrock that was not observed in the boreholes. Concerning the free depth layering, the velocity of the last layer was also fixed to $1500\,\mathrm{m/s}$, but not its depth. Results show that the right depth is retrieved thanks to the ellipticity.

More layers than needed to explain the targets are used to smooth the obtained results and better explore the parameter space. 5 independent runs of 5 different parametrization schemes (5 and 7 layers over a half space, see Fig. 13 and 7, 9 and 10 layers with fixed depth, see Fig. 14) were performed. For further elaborations, the best models of these 25 runs were selected (Fig. 15).

The velocity profiles show 5 first meters with low velocity, around $130 - 140\,\mathrm{m/s}$. A second layer from 5 to $10\,\mathrm{m}$ has slightly higher velocities around $200\,\mathrm{m/s}$. Finally, the layer down to $25\,\mathrm{m}$ shows relatively homogeneous velocities around $275\,\mathrm{m/s}$ Below $25\,\mathrm{m}$, this velocity may increase gradually down to the bedrock. For free layer depth, the bedrock velocity was fixed but not the depth and it happen to be found in the range 30 to $40\,\mathrm{m}$ showing the data constrain the order of magnitude of the depth but the precision is poor.

When compared to the target curves (Fig. 13), the 3 Rayleigh modes are well reproduced, as well as the ellipticity peak. The ellipticity right flank is sharper in the models due to the sharp

velocity contrast. It is however not clear whether the smooth observed H/V curve is realistic or not. Reliable data are lacking to constrain this part of the profile.

This inversion shows that the H/V peak is due to the bedrock interface and not the moraine interface as the correlation in Fig. 7 could suggest. The velocity profile down to the bedrock, very variable in the area, is controlling the peak frequency more than the bedrock depth, which shows only little variation, explaining the distribution of resonance frequencies.

Compared to V_s extracted from the SPT measurements of Tab. 3, these profiles are in agreement. On Fig. 16, the results are compared to 2 profiles (P1 and P5 - P5 has higher velocities at the top) used in the microzonation of EPFL [Résonance, 2006], close to SEPFL station and to the V_s extracted from the SPT measurements. It shows little difference but the results displayed here show that the precision of the used geophysical methods is probably lower than the differences between the profiles used in the microzonation.

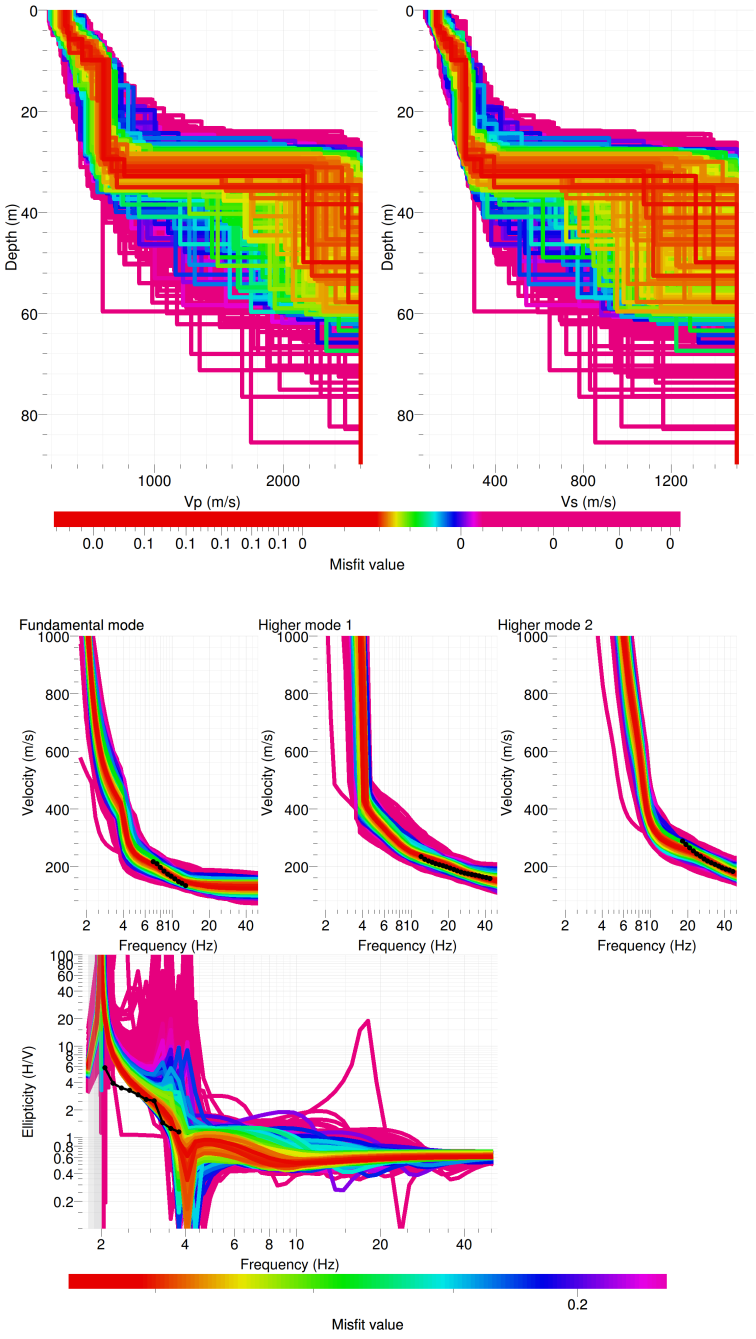

Figure 13: Inverted ground profiles in terms of V_p and V_s (top) and comparison between inverted models and measured Rayleigh and Love modes and corresponding ellipticity, free layer depth strategy.

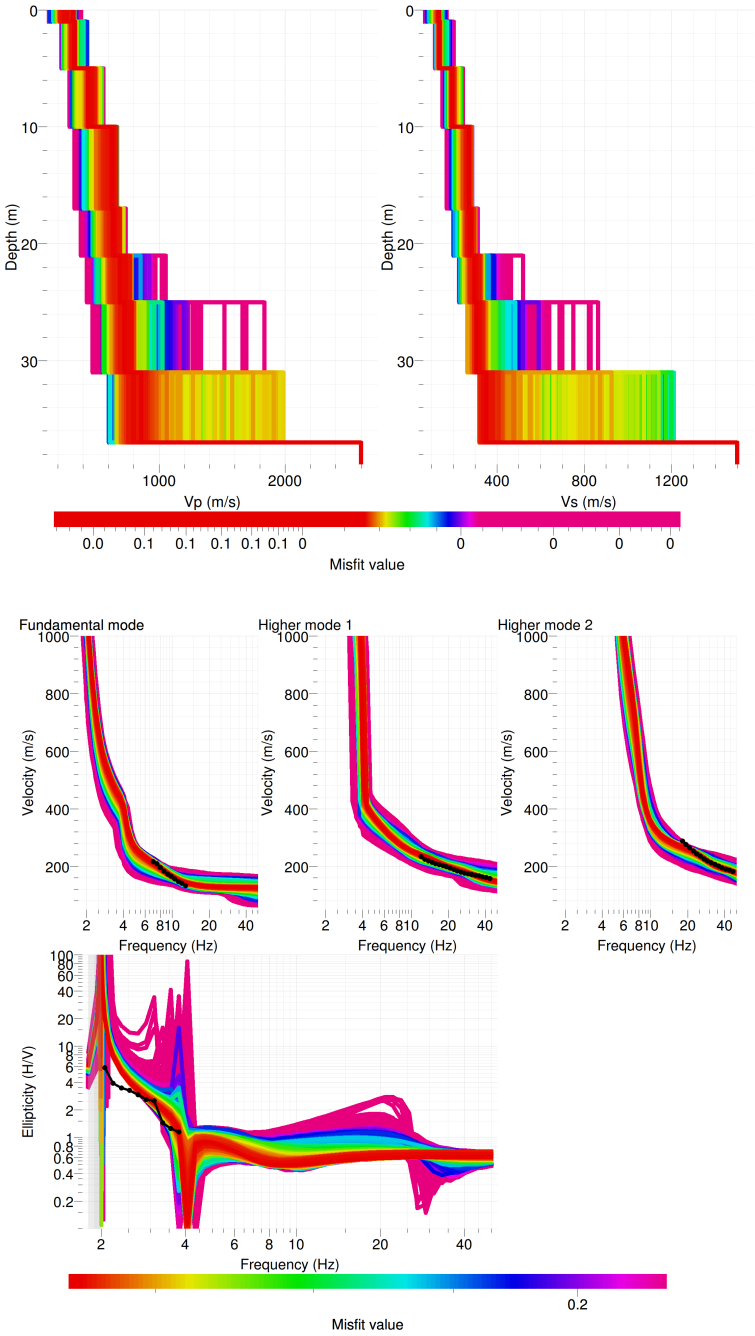

Figure 14: Inverted ground profiles in terms of V_p and V_s (top) and comparison between inverted models and measured Rayleigh and Love modes and corresponding ellipticity, fixed layer depth strategy.

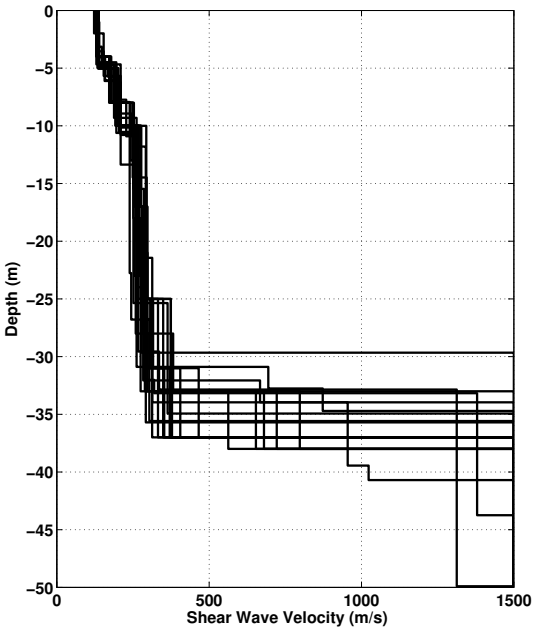

Figure 15: V_s ground profiles for the selected 25 best models.

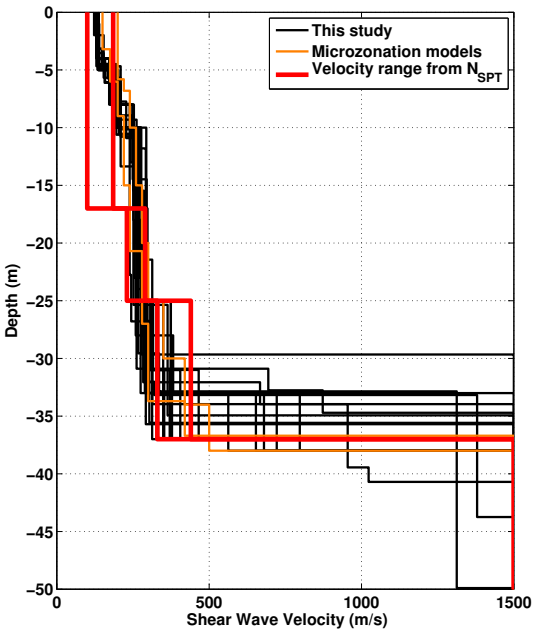

Figure 16: V_s ground profiles for the selected 25 best models compared to 2 of the closest models used for the microzonation and the velocity range obtained from SPT (see Tab. 3).

7.2 Travel time average velocities and soil class

The distribution of the travel time average velocities at different depths was computed from the selected models. The uncertainty, computed as the standard deviation of the distribution of travel time average velocities for the considered models, is also provided, but its meaning is doubtful. $V_{s,30}$ is found to be $224\,\mathrm{m/s}$, meaning the site can be classified as class C in the Eurocode 8 [CEN, 2004] and class D in SIA261 [SIA, 2003]. The map of foundation classes on the website `http://map.bafu.admin.ch/` is also providing a class D at this site.

	Mean (m/s)	**Uncertainty (m/s)**
$V_{s,5}$	137	3
$V_{s,10}$	162	2
$V_{s,20}$	201	4
$V_{s,30}$	224	5
$V_{s,40}$	255	10
$V_{s,50}$	-	-
$V_{s,100}$	-	-
$V_{s,150}$	-	-
$V_{s,200}$	-	-

Table 6: Travel time averages at different depths from the inverted models. Uncertainty is given as one standard deviation from the selected profiles.

7.3 SH transfer function and quarter-wavelength velocity

The quarter-wavelength velocity approach [Joyner et al., 1981] provides, for a given frequency, the average velocity at a depth corresponding to 1/4 of the wavelength of interest. It is useful to identify the frequency limits of the experimental data (minimum frequency in ellipticity and dispersion curves, 2 and $7\,\mathrm{Hz}$, respectively). The results using this proxy show that no data is controlling the results below $26\,\mathrm{m}$ and the dispersion curves constrain the results down to $5\,\mathrm{m}$ only (Fig. 17). In this case, this proxy does not seem to provide relevant results (too conservative) since the 20 first meters seems well constrained, not only by the ellipticity.
Moreover, the theoretical SH transfer function [Roesset, 1970] is computed from the inverted profiles. It is compared to the quarter-wavelength impedance contrast that is a proxy for amplification, that however cannot take resonances into account [Joyner et al., 1981] (Fig. 18). In this case, the SH transfer function shows amplifications up to 10 at the resonance frequencies and upper modes. This very large predicted amplification will be compared to observations at this station.

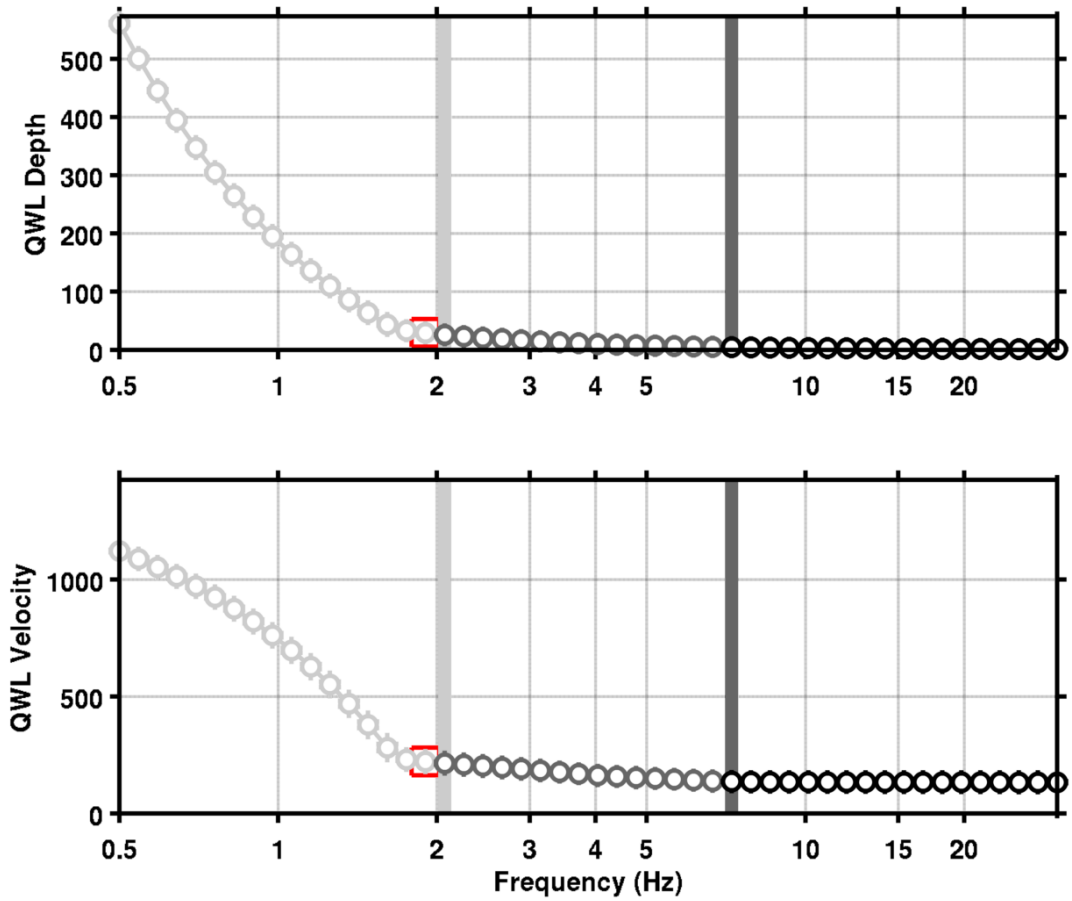

Figure 17: Quarter wavelength velocity representation of the velocity profile. Black curve is constrained by the dispersion curves, grey curve by the ellipticity function, light grey is not constrained by the data. Red square is corresponding to $V_{s,30}$.

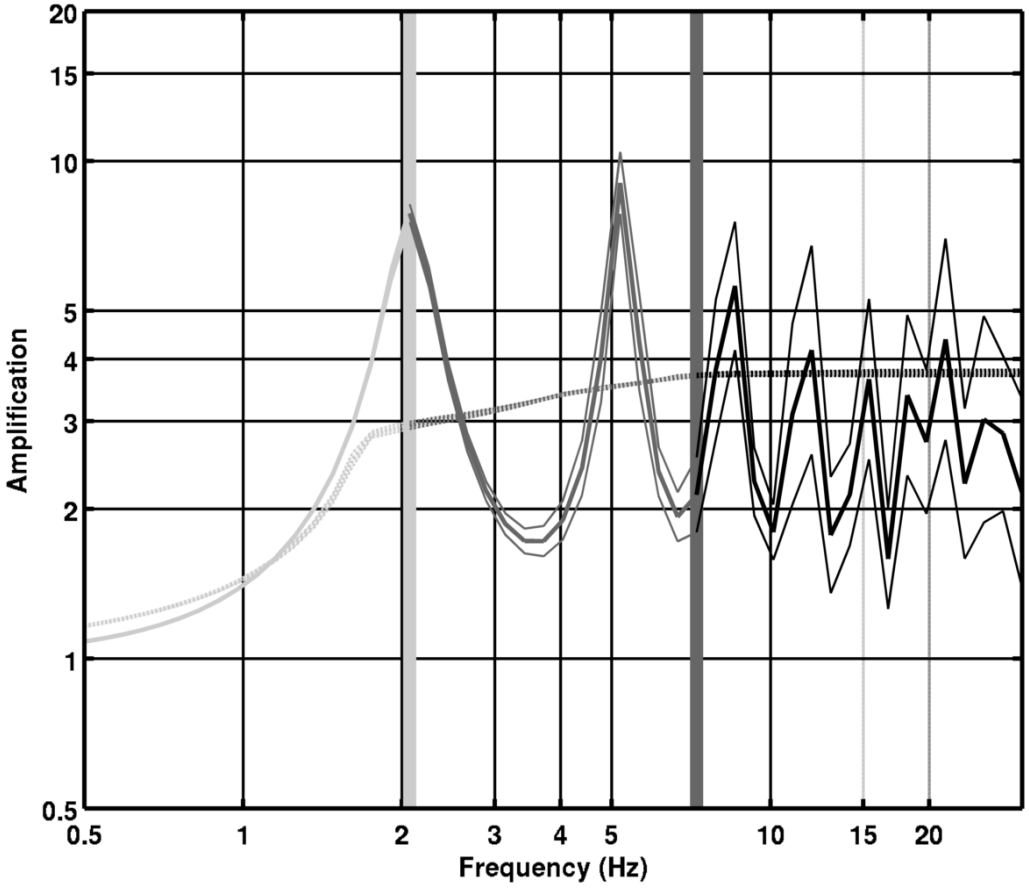

Figure 18: Theoretical SH transfer function (solid line) and quarter wavelength impedance contrast (dashed line) with their standard deviation. Grey scale represents the constraint by the data as in Fig. 17.

8 Conclusions

Thanks to existing geotechnical and geophysical data, as well as new geophysical data, the site of SEPFL station could be characterized in terms of elastic properties. The H/V survey showed the site has a resonance of $1.9\,\mathrm{Hz}$. Using the MASW measurements, a velocity model below SEPFL was extracted. The velocity profiles show 5 first meters with low velocity, around $130 - 140\,\mathrm{m/s}$. A second layer from 5 to $10\,\mathrm{m}$ has slightly higher velocities around $200\,\mathrm{m/s}$. Finally, the layer down to $25\,\mathrm{m}$ shows relatively homogeneous velocities around $275\,\mathrm{m/s}$. Below $25\,\mathrm{m}$, this velocity may increase gradually down to the bedrock, located at $37\,\mathrm{m}$ by the geotechnical survey. $V_{s,30}$ is found to be $224\,\mathrm{m/s}$. The theoretical SH transfer function and impedance contrast of the quarter-wavelength velocity computed from the inverted profiles support a large amplification up to a factor of 10 at the resonance frequencies. Recordings on the new station will allow to validate these simple models.

Appendix: description of datasets for the performed active seismic line

Group A Source type: weight drop
Number of shots: 10 (files 41.dat to 50.dat)
Direction: normal (source A), offset $22\,\mathrm{m}$
Synchronized: YES
Selection: [41 42 44 45 46]
Note: channel 1 of the geophone at offset 11 did not work

Group B Source type: weight drop
Number of shots: 10 (files 51.dat to 60.dat)
Direction: normal (source A), offset $22\,\mathrm{m}$
Synchronized: YES
Selection: [51 57 58 59 60]
Note: traces 52:56 failed (trigger started too late),
channel 1 of the geophone at offset 11 did not work,
channel 3 of the geophone at offset 10 did not work

Group C Source type: weight drop
Number of shots: 9 (files 70.dat to 78.dat)
Direction: reversed (source B)
Synchronized: NO
Selection: [73 74 75 77 78]
Note: on the traces are visible two separate pulses of different amplitude

Group D Source type: sledge hammer
Number of shots: 5 (files 1.dat and 4.dat to 7.dat)
Direction: Normal, offset $21.86\,\mathrm{m}$
Synchronized: NO
Selection: [1 4 6 7]

Acknowledgements

The authors thanks Corinne Lacave from Resonance and Vincent Pellissier from EPFL who provided their data, as well as the Geo2X company who gave precisions on their data. The authors also thank Lea Kiefer for the help during the measurements.

References

Sylvette Bonnefoy-Claudet, Fabrice Cotton, and Pierre-Yves Bard. The nature of noise wavefield and its applications for site effects studies. *Earth-Science Reviews*, 79(3-4): 205–227, December 2006. ISSN 00128252. doi: 10.1016/j.earscirev.2006.07.004. URL http://linkinghub.elsevier.com/retrieve/pii/S0012825206001012.

CEN. *Eurocode 8: Design of structures for earthquake resistance - Part 1: General rules, seismic actions and rules for buildings*. European Committee for Standardization, en 1998-1: edition, 2004.

William B. Joyner, Richard E. Warrick, and Thomas E. Fumal. The effect of Quaternary alluvium on strong ground motion in the Coyote Lake, California, earthquake of 1979. *Bulletin of the Seismological Society of America*, 71(4):1333–1349, 1981.

Katsuaki Konno and Tatsuo Ohmachi. Ground-Motion Characteristics Estimated from Spectral Ratio between Horizontal and Vertical Components of Microtremor. *Bulletin of the Seismological Society of America*, 88(1):228–241, 1998.

Yutaka Ohta and Noritoshi Goto. Empirical shear wave velocity equations in terms of characteristic soil indexes. *Earthquake Engineering & Structural Dynamics*, 6(2):167–187, March 1978. ISSN 00988847. doi: 10.1002/eqe.4290060205. URL http://doi.wiley.com/10.1002/eqe.4290060205.

V. Poggi, D. Fäh, and D. Giardini. Time-Frequency-Wavenumber Analysis of Surface Waves Using the Continuous Wavelet Transform. *Pure and Applied Geophysics*, June 2012. ISSN 0033-4553. doi: 10.1007/s00024-012-0505-5. URL http://www.springerlink.com/index/10.1007/s00024-012-0505-5.

Résonance. Site EPFL Microzonage sismique spectral. Technical report, Ecole Polytechnique Fédérale de Lausanne (EPFL), Geneva, 2006.

J.M. Roesset. Fundamentals of soil amplification. In R. J. Hansen, editor, *Seismic Design for Nuclear Power Plants*, pages 183–244. M.I.T. Press, Cambridge, Mass., 1970. ISBN 978-0-262-08041-5. URL http://mitpress.mit.edu/catalog/item/default.asp?ttype=2\&tid=5998.

SIA. *SIA 261 Actions sur les structures porteuses*. Société suisse des ingénieurs et des architectes, Zürich, sia 261:20 edition, 2003.

Marc Wathelet. An improved neighborhood algorithm: Parameter conditions and dynamic scaling. *Geophysical Research Letters*, 35(9):1–5, May 2008. ISSN 0094-8276. doi: 10.1029/2008GL033256. URL http://www.agu.org/pubs/crossref/2008/2008GL033256.shtml.